Apolipoprotein A-I mimetic peptide helix number and helix linker influence potentially anti-atherogenic properties

Geoffrey D. Wool, Catherine A. Reardon, and Godfrey S. Getz[1]

The University of Chicago, Department of Pathology, Chicago, IL

Abstract We hypothesize that apolipoprotein A-I (apoA-I) mimetic peptides better mimicking the punctuated α-helical repeats of full-length apoA-I are more anti-inflammatory and anti-atherogenic. This study compares a monomeric apoA-I mimetic helix to three different tandem helix peptides in vitro: 4F (18 mer), 4F-proline-4F (37 mer, Pro), 4F-alanine-4F (37 mer, Ala), and 4F-KVEPLRA-4F [the human apoA-I 4/5 interhelical sequence (IHS), 43 mer]. All peptides cleared turbid lipid suspensions, with 4F being most effective. In contrast to lipid clearance, tandem peptides were more effective at remodeling mouse HDL. All four peptides displaced apoA-I and apoE from the HDL, leaving a larger particle containing apoA-II and peptide. Peptide-remodeled HDL particles show no deficit in ABCG1 cholesterol efflux despite the loss of the majority of apoA-I. Tandem peptides show greater ability to efflux cholesterol from lipid-loaded murine macrophages, compared with 4F. Although 4F inhibited oxidation of purified mouse LDL, the Ala tandem peptide increased oxidation. We compared several tandem 4F-based peptides with monomeric 4F in assays that correlated with suggested anti-inflammatory/anti-atherogenic pathways. Tandem 4F-based peptides, which better mimic full-length apoA-I, exceed monomeric 4F in HDL remodeling and cholesterol efflux but not LDL oxidation protection. In addition, apoA-I mimetic peptides may increase reverse cholesterol transport through both ABCA1 as well as ABCG1 pathways.—Wool, G. D., C. A. Reardon, and G. S. Getz. **Apolipoprotein A-I mimetic peptide helix number and helix linker influence potentially anti-atherogenic properties. *J. Lipid Res.* 2008.** 49: **1268–1283.**

Supplementary key words synthetic peptides • 4F • cholesterol • metabolism • oxidation

HDL has been directly shown to be anti-atherogenic in animal models of atherosclerosis (1). In meta-analysis, each 1 mg/dl increase in human HDL-cholesterol (HDL-C) is associated with a 2–3% decrease in the risk of future coronary heart disease (CHD) (2). Pharmacologically enhancing the serum level of HDL, or the particle's anti-atherogenic properties, in patients still at risk of CHD even after being adequately treated with statins has been called the next frontier in the prevention of CHD (3). Treating humans with phosphoplipid discs containing apolipoprotein A-I (apoA-I), the major protein of HDL, increases HDL-C and reverse cholesterol transport (RCT) (4) and decreases coronary atheroma volume (5).

The apoA-I sequence has a repeating tandem amphipathic α-helical motif (6). 18 mer peptide mimetics of apoA-I, which represent a single averaged amphipathic α-helical motif without an interhelical sequence (IHS), have been investigated, first as models for apoA-I in vitro and subsequently as a treatment for atherosclerosis. The original apoA-I mimetic peptide (18A) was modified by N- and C-terminal capping to increase helical rigidity and by substitution of two phenylalanines for the two leucines to increase its hydrophobicity, making the 4F peptide (7). Gavage of mice with D-amino acid containing 4F (D4F) resulted in the formation of anti-inflammatory pre-β HDL particles (8), a process hypothesized to be due to peptide-mediated HDL remodeling.

In addition to HDL remodeling, D4F has been shown to promote in vitro cholesterol efflux and in vivo murine RCT as well as decrease atherosclerosis (8, 9). Intraperitoneal (IP) administration of L-amino acid-based 4F has also been shown to improve vascular reactivity (10). The L-amino acid version of the related mimetic peptide 5F has been shown to decrease atherosclerosis in C57BL/6 mice when administered IP (11).

Although the apoA-I mimetic peptide 4F is anti-inflammatory and anti-atherogenic, a detailed understanding of its influence on HDL metabolism is lacking. It is unknown whether a peptide that better mimicked the structure of lipidated apoA-I would have increased potency or efficacy. Sequence analysis has suggested that the true paradigmatic repeat in apoA-I is a 44 mer: two tandem 22 mers disrupted by their IHS, which contains a proline

This work was supported by the National Heart, Lung, and Blood Institute, Grant HL-68661. G.D.W. has received support from the National Institute of Child Health and Human Development, Grant HD-007009, Graduate Training in Growth and Development, the Francis L. Lederer Foundation Scholarship Fund, and an American Heart Association pre-doctoral fellowship.

Manuscript received 27 November 2007 and in revised form 28 January 2008 and in re-revised form 4 March 2008.

Published, JLR Papers in Press, March 5, 2008.
DOI 10.1194/jlr.M700552-JLR200

[1] To whom correspondence should be addressed.
e-mail: getz@bsd.uchicago.edu

kink (12). Previous peptide studies utilizing the 18A peptide backbone, which is not anti-atherosclerotic, have shown that proline-kinked tandem mimetic peptides have increased lipid affinity, helicity when lipid-associated, and apoA-I displacement abilities, compared with monomeric 18A (13–15).

The lipid-free Δ1-43 apoA-I crystal structure shows a tertiary structure with 10 helices, the interhelical punctuations of which include all six prolines in the protein (16). The central location of the proline residue between the tandem α-helical repeats results in a mildly concave hydrophobic surface (17) that is well suited to fit the geometry of the curved HDL surface.

Despite the recent determination of a disparate lipid-free apoA-I structure (18), significant evidence continues to argue for the proline-punctuated tandem α-helical structure of lipid-associated apoA-I. The lipid-free Δ1-43 apoA-I crystal structure has been widely accepted and corroborated as a good model of the structure of lipid-associated apoA-I (17, 19–21), even by the authors of the lipid-free full-length apoA-I crystal structure report (18). Additionally, the full-length lipid-free apoA-I crystal structure shows that four out of the five α-helices in exon four contain a proline residue at the helix start or termination, or within one helix turn of the start or termination.

Overall, significant evidence continues to argue for the proline-punctuated tandem α-helical lipid-associated apoA-I structure. Given the inability of mimetic peptides to significantly alter their structure, unlike full-length apoA-I, peptides must be modeled on the lipid-associated structure. Several studies have demonstrated that human apoA-I on reconstituted discoidal HDL adopts loop structures corresponding to proline-containing IHSs (22, 23). This investigation aims to create an apoA-I mimetic peptide that better models lipid-associated apoA-I; we hypothesize that this peptide will have increased anti-atherosclerotic abilities compared with the 4F monomer.

The peptides utilized in this study are listed in **Table 1**; all except the monomer 4F are described as tandem helix peptides. The putative IHSs in human apoA-I contain a proline in 7 out of 10 cases. The helix 7/helix 8 IHS contains an alanine and a diglycine motif but no proline. In the Δ1-43 apoA-I crystal structure, the average proline-containing IHS adopts a 39.9° interhelical angle, whereas 7/8 IHS adopts an angle of 12–18° (16). These data demonstrate the importance of the proline versus other amino acid linkers for tandem peptide comparison. Therefore, we have chosen to compare a proline to an alanine linker. A final tandem peptide linked by the proline-containing human 4/5 IHS was chosen as a linker because *1*) it contains the canonical proline kink, *2*) we have shown that it is important in determining HDL subspecies association (23a), *3*) the 4/5 IHS sequence differs between species that have a monophasic (mouse, rabbit, pig) and biphasic (human) HDL profile, and *4*) the 4/5 IHS is within the putative apoA-I flexible hinge domain (24). Solely changing the helix linker in these tandem peptides creates significant structural differences (25) without introducing any other confounding changes.

The peptides investigated are not exact representations of apoA-I helix–IHS-helix segments. The choice was made to use the known anti-atherosclerotic backbone 4F, because one goal of this investigation is to determine the best potential tandem peptide for comparison to 4F in future atherosclerosis studies.

We have taken an integrated approach to studying these tandem mimetics and have compared their abilities in a variety of assays of pathways that were correlated with atherosclerosis inhibition by the Fogelman group (8, 26). This will allow future correlation between the peptide remodeling of lipid and HDL, cholesterol efflux, and LDL oxidation prevention to in vivo atherosclerosis prevention. We hypothesized that apoA-I mimetics replicating the punctuated tandem repeat of apoA-I would be more effective than 4F in a variety of in vitro assays that correlate with known anti-atherosclerotic pathways.

METHODS

Peptides

Peptides were synthesized from L-amino acids using standard Fastmoc solid-phase chemistry on an Applied Biosciences (Foster City, CA) peptide synthesizer. All peptides were acetylated at their N terminus with acetic anhydride and amidated at the C terminus with a Fmoc-Rink Amide resin (Anaspec, San Jose, CA). After trifluoroacetic acid cleavage, peptides were purified by reverse-phase (RP)-HPLC on a preparative C18 column using water-acetonitrile gradients in 0.1% (v/v) trifluoracetic acid at a flow rate of 10 ml/min. Purity was confirmed by analytical RP-HPLC. Molecular mass was confirmed by mass spectrometry. Peptide concentration was determined by extinction coefficient (ε_{280} = 7,300 M^{-1} cm^{-1} for 4F and 14,600 M^{-1} cm^{-1} for tandem helix peptides). Peptides were stored lyophilized at −20°C until use. None of the peptides discussed in this pa-

TABLE 1. Peptide helix number and linker influence hydrophobicity

Peptide	Sequence (L-amino acids)	Acetonitrile for elution off C18 column
		%
4F (4F)	Ac-DWFKAFYDKVAEKFKEAF-NH2 (18 mer)	51
4F-Hu apoA-I 4/5 Interhelical sequence-4F (IHS)	*4F*-KVEPLRA-*4F* (43 mer)	52
4F-Pro-4F (Pro)	*4F*-P- *4F* (37 mer)	56
4F-Ala-4F (Ala)	*4F*-A- *4F* (37 mer)	60

apoA-I, apolipoprotein A-I.

per formed precipitates upon extended storage at 4°C in PBS (4F was stored at a maximum concentration of 274 μM, whereas the tandems were stored at a maximum of 137 μM).

Lipoproteins

Mouse lipoproteins were isolated by ultracentrifugation of pooled serum from mice with wild-type (wt) apolipoprotein genotypes. Mouse LDL (moLDL) was isolated at a density of 1.019–1.063 g/ml and mouse HDL (moHDL) at a density of 1.063–1.21 g/ml. Human LDL (density of 1.019–1.063 g/ml) was acetylated with acetic anhydride in a saturated solution of sodium acetate on ice, as described (27, 28). Acetylation was monitored by qualitative ninhydrin assay. Acetylated LDL (acLDL) was dialyzed extensively before use.

Lipid clearance

Dimyristoylphosphatidylcholine (DMPC) and 1-palmitoyl-2-oleoyl-*sn*-glycerol-3-phosphocholine (POPC) multilamellar vesicles were prepared by vortexing in TBS until turbid and then filtered using a 0.2 μm polyethersulfone filter. Incubations were carried out at room temperature at various lipid:peptide mass ratios. Turbidity was monitored at optical density (OD) 490 nm using a BioTek (Winooski, VT) μQuant microplate spectrophotometer.

Electron microscopy

DMPC was prepared in 10 mM phosphate buffer (pH 7.4) and filtered as above. Lipid-free peptide in 10 mM phosphate buffer (pH 7.4) was added to 1 mg/ml turbid DMPC for a final peptide concentration of 0.12 mg/ml. After 1 h of clearance, 5 μl of the product was applied to a glow-discharged, 400-mesh, carbon-coated support film and stained with 2% phosphotungstic acid. Images were taken on a Tecnai F30 electron microscope at the University of Chicago at 137,200× magnification, and at least 99 discs were quantified using OpenLab 3.1.5 software (Improvision Inc., Lexington, MA).

HDL remodeling

Peptide and moHDL were incubated at 37°C for 20 min with gentle shaking. Agarose electrophoresis was carried out in 0.7% agarose gels in 25 mM tricine/3 mM calcium lactate buffer. Native exponential gradient PAGE separation was carried out in 2–36% native acrylamide gels in tris-boric acid-EDTA buffer.

Agarose gels and SDS-PAGE gels were transferred to Immobilon (Millipore, Bedford, MA) membranes for 1 hr. Native PAGE gels were transferred to Immobilon membranes for 20 h at 400 mA. Membranes were blocked in 5% nonfat dry milk in TBS-Tween. Primary immunoblotting for apoA-I (polyclonal rabbit α mouse, 1:20,000), apoA-II [polyclonal rabbit α mouse (Biodesign K23400R, Saco, ME), 1:1000], and apoE (polyclonal rabbit α rat, 1:1000) was carried out for 1 h, and the secondary [affinity-purified HRP-linked polyclonal goat α rabbit IgG (Sigma A-4914, St. Louis, MO), 1:1000] was carried out for 1 h. Membranes were visualized by enhanced chemiluminescence, and digital images were captured using AlphaImager (Alpha Innotech, San Leandro, CA). Percent remodeling was determined using the spot densitometry feature of the FluoroChem v 2.0 program.

Remodeled particles were separated by single-spin ultracentrifugation (38,000 rpm/66 h/15°C/no brake) using 10–20% NaBr gradients (29).

Cholesterol was measured using Roche (Indianapolis, IN) enzymatic assay, phospholipid using Wako (Richmond, VA) phospholipids B enzymatic assay, and protein using Bio-Rad Protein (Hercules, CA) assay (500-0006) according to the manufacturers' protocols.

Cholesterol efflux

The macrophage efflux procedure was modified from that reported by Phillips and colleagues (30). J774A.1 cells (TIB-67; American Type Culture Collection, Manassas, VA) were cultured to 80–90% confluency in DMEM (4.5 g/l glucose) with 10% FBS at 5% CO_2. Cells were then incubated with 1% FBS, 2 μg/ml Sandoz (Sigma) ACAT inhibitor, 25 μg/ml acLDL (by protein), and 3 μCi/ml ^{3}H-cholesterol in DMEM for 48 h followed by 12 h in FBS-free DMEM with 0.2% (w/v) BSA, and 2 μg/ml Sandoz ACAT inhibitor, with or without 0.3 mM 8-(4-Chlorophenylthio)-adenosine-3',5'-cyclic monophosphate (CPT-cAMP) (Sigma). Peptides at concentrations of 0–25 μg/ml were then applied in FBS-free DMEM for 4 h. Cell-free media was collected, and the cells were washed twice with PBS.

Media was extracted using a 1:1:8 ratio of media:ice-cold ethanol:hexane, and the top layer was collected and dried. Cellular lipids were extracted three times using 500 μl per well of 3:2 hexane:isopropanol. Extraction solvents were dried, ^{3}H-cholesterol was measured by scintillation counting using Econofluor (Perkin-Elmer, Waltham, MA), and efflux was quantified as media counts as a percent of [media + cell] counts.

BHK cells with the human ABCG1 (huABCG1) gene expressed with the GeneSwitch system (Invitrogen, Carlsbad, CA) were a generous gift from J. Oram (University of Washington). Cells were maintained in DMEM (4.5 g/l glucose) with 10% FBS at 5% CO_2 with 100 μg/ml zeocin. The huABCG1 BHK efflux procedure was modified from that reported by Vaughan and Oram (31). At ~70% confluency, cells were washed and incubated with 10% FBS and 3 μCi/ml ^{3}H-cholesterol in DMEM for 48 h. The cells were then incubated for 18 h in FBS-free DMEM with 1 mg/ml BSA with or without 10 nM mifepristone. HDL particles were then applied in FBS-free DMEM with 1 mg/ml NEFA-free BSA for 4 h. To obtain peptide-modified moHDL particles, 0.237 mg/ml moHDL (protein) was incubated with PBS (wt moHDL), 18.2 μM 4F (4F-associated moHDL), 182.3 μM 4F (4F-remodeled moHDL), 3.37 μM IHS (IHS-associated moHDL), or 33.67 μM IHS (IHS-remodeled moHDL) for 20 min at 37°C with gentle shaking. The particles were separated from free peptide/protein by ultracentrifugation on a 10–20% NaBr gradient. Peak fractions representing mature particles were pooled for each condition. The increase in protein:total cholesterol (w:w) ratio for the postcentrifugation pooled 4F-associated moHDL, 4F-remodeled moHDL, IHS-associated moHDL, and IHS-remodeled moHDL was 1.1-, 1.7-, 1.1-, and 1.6-fold, respectively, compared with wt moHDL. The media and cellular lipids were collected and extracted as described above.

LDL oxidation

moLDL was extensively dialyzed against PBS before use in the oxidation assay. Incubations of 20 μg/ml moLDL with 10 μg/ml peptide and 50 μM copper sulfate pentahydrate or 300 U/ml lipoxygenase type IB (Sigma) were carried out at room temperature. Oxidation was assayed by conjugated diene formation at OD 234 nm using a Beckman DU60 (Fullerton, CA) spectrophotometer with kinetics softpack.

To evaluate the effects of peptide on LDL oxidation, three independent experiments were quantified for each oxidation method. For copper oxidation, slopes of the linear phase were quantified by determining the segment of the curve (containing at least eight time points) that had the greatest linear regression r^2 value. The lag times were defined as the duration from

time zero to the point at which the linear phase began. Total oxidation was the difference between the minima and maxima of the curves. For lipoxygenase oxidation, slopes of the linear phase were quantified by linear regression of the segment of the curve (from ≤130 min until the conclusion of the experiment) that had the greatest r^2 value.

Statistics

Data are presented as average ± standard deviation. Statistical significance was tested using Student's *t*-test.

RESULTS

Tandem apoA-I mimetic peptides are more hydrophobic than monomeric 4F

Mimetic peptide elution off a preparative C18 HPLC (Table 1) demonstrated not unexpectedly that doubling the amphipathic α-helix length increased peptide hydrophobicity, compared with monomeric 4F. The effect of helix number was greatly influenced by the tandem helix linker, however. The Ala tandem, containing a linker known to be a canonical helix propagator, showed the greatest hydrophobicity. This is probably due to both its greater helix length and the decreased propensity of the peptide to kink back onto itself, as is believed to occur with the proline-containing tandem peptides (Pro and IHS). The imino acid proline disrupts the i to $i + 3$ hydrogen bonding of an α-helix and promotes the formation of helix kinks (12), as demonstrated by the average ~23° kink induced by a proline residue in a right-handed α-helix (32). The decreased hydrophobicity of IHS compared with Pro is probably due to the self-associating behavior of the peptide containing the KVEPLRA IHS, as has been described for a similar tandem peptide containing the identical IHS (25).

4F shows the quickest and most complete clearance of DMPC, whereas the Ala tandem causes no net change in turbidity

To determine the relative lipid remodeling abilities of these apoA-I mimetic peptides, they were mixed with turbid DMPC suspensions, and the clearance of the suspension by formation of lipid/peptide particles was monitored by light scattering. Faster clearance demonstrates greater ability to interact with phospholipids to the exclusion of peptide self-association (26). The order of lipid clearance by various 18 mer apoA-I mimetic peptides (33) appears to correlate with their anti-inflammatory ability in the arterial wall coculture model (26). A 17.5:1 ratio (data not shown) and an 8.3:1 ratio (**Fig. 1A**) showed similar trends of kinetics and overall clearance. All four peptides cause rapid DMPC clearance, with 4F being the fastest (Fig. 1A). The nearly complete initial clearance of lipid by 4F has previously been shown by Datta et al. (33), who demonstrated that 4F cleared DMPC nearly as quickly as Triton X-100. The initial rapid clearance of DMPC by Ala, followed by a slower increase in turbidity, is probably due to the long unbroken α-helix causing fusion of the newly formed particles. Both proline-containing tandems caused similar overall clearance, but IHS had a faster initial clearance than Pro. The proline-containing tandems approach the overall clearance of 4F at longer clearance times, but they are much less effective than 4F on a kinetic basis.

An 8.3:1 (w:w) ratio of POPC:peptide confirmed the superior lipid-remodeling ability of 4F relative to the tandem peptides, inasmuch as only 4F was able to appreciably clear this more physiologic lipid (data not shown). Compared with POPC, DMPC is less resistant to clearance, because its short, 14-carbon acyl chains create lattice defects at the gel-to-liquid crystal phase transition of bilayers (34).

ApoA-I mimetic peptides interact with turbid phospholipids to form discoidal complexes, with the peptides wrapping around the side of the disc to shield the phospholipid acyl tails in a manner analogous to a belt (35). Electron microscopy studies demonstrate that all peptides were able to remodel the DMPC suspension from vesicles whose average diameter was 325 nm (data not shown) into small discs after 1 h of clearance (Fig. 1B). The identification of the remodeled particles as discs is based upon the similar average lengths of the long axes of both the linear and circular structures in the photomicrographs. We infer that these represent the same population of particles either viewed on edge or en face, respectively.

4F and the proline-containing tandems (Pro and IHS) formed extensive rouleaux. The Ala peptide is unique in that it forms a limited number of discs of various sizes without extensive stacking, together with circular structures that often contain an area of increased density in the center, creating a seemingly "doughnut"-shaped particle. The lack of Ala disc stacking is probably the cause of the increased turbidity of the Ala DMPC clearance reaction, inasmuch as the particles disperse and prevent the passage of light. We hypothesize that the range of particle shapes and sizes caused by the Ala peptide is indicative of particle fusion and the lack of an equilibrated population. Given this constraint, only the particles formed by 4F, IHS, and Pro have been quantified.

Quantification of the peptide-lipid disc's long axis shows that 4F creates larger discs on average than the proline-containing tandem peptides, which behave similarly regardless of their linker (Fig. 1C). We do not believe this slight difference in average disc size is relevant to the difference in lipid clearance (Fig. 1A), because the size difference between the discs is on the order of ~5 nm, whereas the size difference between the initial lipid particles and the disc products is ~300 nm.

The size distribution of discs formed from tandem peptides shows a unimodal distribution, with the rank order of the disc distribution peak being IHS < Pro (Fig. 1D). The difference in particle size between IHS and Pro is probably due to salt bridges in the KVEPLRA IHS (25) causing a greater bend between the tandem helices than a lone proline and thereby limiting the formation of larger lipid particles.

The 4F particle size distribution, on the other hand, showed three distinct peaks. The diameter of the majority of the particles was between 30 and <35 nm, similar to the peak size of the Pro particles, whereas two lesser

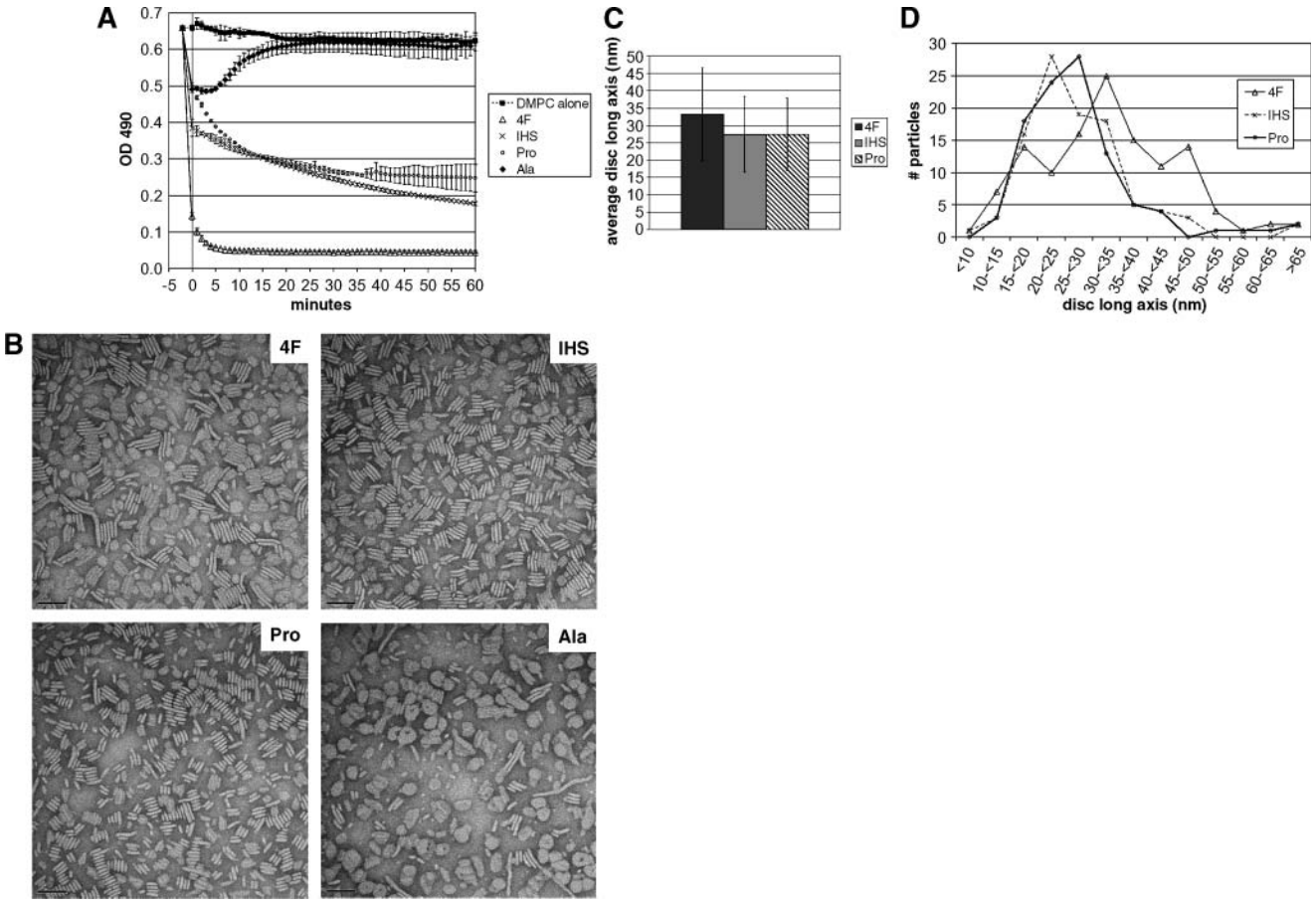

Fig. 1. Dimyristoylphosphatidylcholine (DMPC) clearance by apolipoprotein A-I (apoA-I) mimetic peptides. A: Kinetics of peptide clearance. Lipid-free peptide in TBS was added at 0.12 mg/ml to a 1 mg/ml turbid DMPC suspension in TBS. The clearance reactions were allowed to proceed for 1 h at room temperature. Owing to the speed of the initial clearance, the peptide-containing reactions have been extrapolated back to the initial DMPC value (line). B: Negative-stain electron microscopy of peptide-DMPC particles. Lipid-free peptide in 10 mM phosphate buffer (pH 7.4) was added at 0.12 mg/ml to a 1 mg/ml turbid DMPC suspension in phosphate buffer. The clearance reactions were allowed to proceed for 1 h, and the product was applied to the grid. Scale bar represents 50 nm. Images were taken at 137,200× magnification. C: Size analysis. Data is represented as mean ± SD. D: Size distribution of ≥ 99 peptide:lipid discs by measurement of their long axis. Only those peptides that formed equilibrated populations of discs are included [L4F, Pro, interhelical sequence (IHS)].

peaks occurred at 15–<20 nm and 45–<50 nm. The ability of 4F to create distinct populations of lipid particles at increments of ~15 nm, corresponding to sizes roughly 0.5 times, 1 time, and 1.5 times the size of the Pro particle peak, suggests that the monomeric 4F may be creating particles of increasing size by increasing the number of peptides per particle.

ApoA-I mimetic peptides displace apoA-I from moHDL

4F, a proven anti-atherosclerotic mimetic peptide, has been shown to shift apoA-I from α-migrating (HDL-associated) to pre-β-migrating (lipid-free/poor apoA-I). The displacement of apoA-I correlates with the anti-atherosclerotic effect (26), presumably owing to the ability of pre-β apoA-I to *1*) extract cholesterol from arterial wall foam cells (36), *2*) activate LCAT to esterify cholesterol to generate spherical HDL and act as a lipoprotein cholesterol sink (37), and *3*) scavenge oxidized lipids away from pro-inflammatory LDL (38). To determine whether the doubling of amphipathic helix number increases the apolipoprotein-displacing ability of the mimetic peptides, increasing amounts of peptides were incubated with purified moHDL for 20 min at 37°C to allow remodeling. The concentration of purified moHDL used for this reaction (6.2 μg/ml HDL protein) is equivalent to 0.32 mg/dl HDL-C.

The products were separated by agarose electrophoresis, and the migration of apoA-I was determined by immunoblot (**Fig. 2**). All four peptides, at concentrations between 1 μM and 5.2 μM, displaced the majority of apoA-I from the α-migrating mature HDL position into the pre-β position. The tandems appeared to show a slightly greater potency of remodeling, though the nature of agarose protein electrophoresis did not allow precise quantitation. In contrast, human apoA-I only began showing displacement of apoA-I from moHDL at >9 μM (data not shown).

Both discoidal HDL and lipid-free apoA-I migrate at a pre-β position (36). Therefore, the identical pre-β electrophoretic mobility of recombinant lipid-free mouse apoA-I and a proportion of mouse plasma apoA-I (Fig. 2) precludes an unambiguous interpretation as to the exact state of displaced apoA-I.

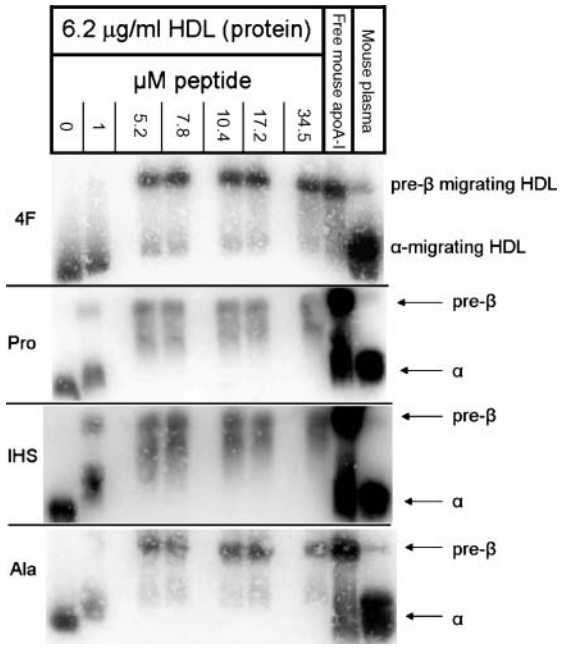

Fig. 2. Peptide-remodeled mouse HDL (moHDL) separated by agarose. Purified moHDL was incubated with increasing amounts of lipid-free peptide at 37°C for 20 min. The agarose gel was transferred and probed with anti-apoA-I antibody.

Tandem peptides show more-potent displacement of apoA-I from moHDL and form larger remodeled lipoproteins

To better define the state of displaced apoA-I, allow quantification, and determine the composition of the apoA-I-less spherical moHDL after remodeling, similar peptide remodeling experiments were analyzed using native PAGE. Coomassie-stained gels (**Fig. 3A**) demonstrated remodeling by the appearance of a protein doublet of ~7.15 nm diameter. Comparison of the Coomassie-stained gels and the anti-apoA-I immunoblots (Fig. 3A) showed the ~7.15 nm-diameter protein to be apoA-I. This migrated at the same size as lipid-free recombinant mouse apoA-I. Coomassie-stained gels showed detectable moHDL remodeling at ~4 μM for tandem peptides, whereas monomeric 4F showed detectable remodeling at 29 μM.

In addition to the small-diameter doublet of remodeled apoA-I, a second product of peptide-HDL remodeling was demonstrated by Coomassie stain of native PAGE. Unremodeled moHDL showed an average diameter of 9.9 nm. moHDL remodeling by 4F, IHS, or Pro produced a slightly larger discrete lipoprotein as visualized by Coomassie stain (Fig. 3A). 4F increased the diameter by 0.08 nm, IHS by 2.65 nm, and Pro by 1.56 nm; all of these slightly enlarged particles still fall within the human HDL size range (39). In contrast, the Ala tandem produced a range of sizes of product particles, a significant proportion of which were as big as a dense LDL particle, resulting in a diameter increase of more than 7 nm (Fig. 3A).

The anti-apoA-I immunoblots showed detectable remodeling of moHDL between 1 μM and 5 μM for all peptides, demonstrating a concentration identical to that seen for immunoblotting of agarose gels. As a qualitative analysis of the peptide concentration dependence of moHDL remodeling, the ECL signals representing free apoA-I- and HDL-bound apoA-I immunoreactivity in each lane were analyzed by spot densitometry from duplicate native PAGE immunoblots. The three tandem peptides displaced apoA-I from HDL in close to an all-or-none phenomenon, showing a hyperbolic concentration curve when quantifying the free apoA-I (~7.1 nm diameter) immunoreactivity as percent of total immunoreactivity per lane (Fig. 3B). Concentrations of tandem peptides of >14 μM were associated with more than 90% of total apoA-I immunoreactivity migrating in the free protein position. This demonstrates the almost total lack of apoA-I on tandem peptide-remodeled mature HDL particles. In contrast, 4F-remodeled moHDL retained roughly half of total apoA-I immunoreactivity, even at 4F concentrations up to 57 μM (Fig. 3B).

ApoA-I mimetic peptides preferentially displace apoA-I and apoE to create apoA-II/peptide-containing lipoproteins

The relative preference of apoA-I mimetic peptides to displace apoA-I rather than apoA-II from HDL has been described previously by others using 18A-based peptides (14). To better explore the displacement of apolipoproteins from HDL and the properties of the remodeled moHDL particle, moHDL was remodeled using concentrations of peptide sufficient to reach the plateau phase of the remodeling curve (Fig. 3B) and nearly complete displacement of apoA-I. This corresponded to 33.67 μM for the three tandems and 182.3 μM for 4F. This high concentration of 4F was experimentally determined to be necessary for complete displacement of apoA-I (data not shown). Following the remodeling reaction, the peptide + moHDL solution was subjected to density gradient ultracentrifugation.

To confirm the formation of an HDL after mimetic peptide remodeling, cholesterol and phospholipid (**Fig. 4A**) distributions in density gradient fractions were assayed. 4F, IHS, and Pro remodeling did not significantly change the density distribution of lipid from that seen with unremodeled moHDL, whereas the Ala tandem created a lipoprotein whose density is similar to that of a small, dense LDL particle.

To determine the apoprotein composition of these density fractions, they were applied to SDS-PAGE and Coomassie stained. Unremodeled moHDL showed the peak of both apoA-I and apoA-II distribution at the 1.125 g/ml fraction, with little of either protein found in the free protein fractions (Fig. 4B, C). On the other hand, all peptides displaced apoA-I (Fig. 4B) and apoE (data not shown and Fig. 4D) into the free protein fractions. Ultracentrifugation of peptide-remodeled moHDL and chloroform-delipidated moHDL (data not shown) showed an identical appearance of apoA-I in density fractions from >1.125 g/ml to 1.25 g/ml. This, along with the similar migration of HDL-derived remodeled apoA-I and recombinant apoA-I on native PAGE (Fig. 3A), suggests that mimetic peptides displace most of the apoA-I as essentially lipid-free protein.

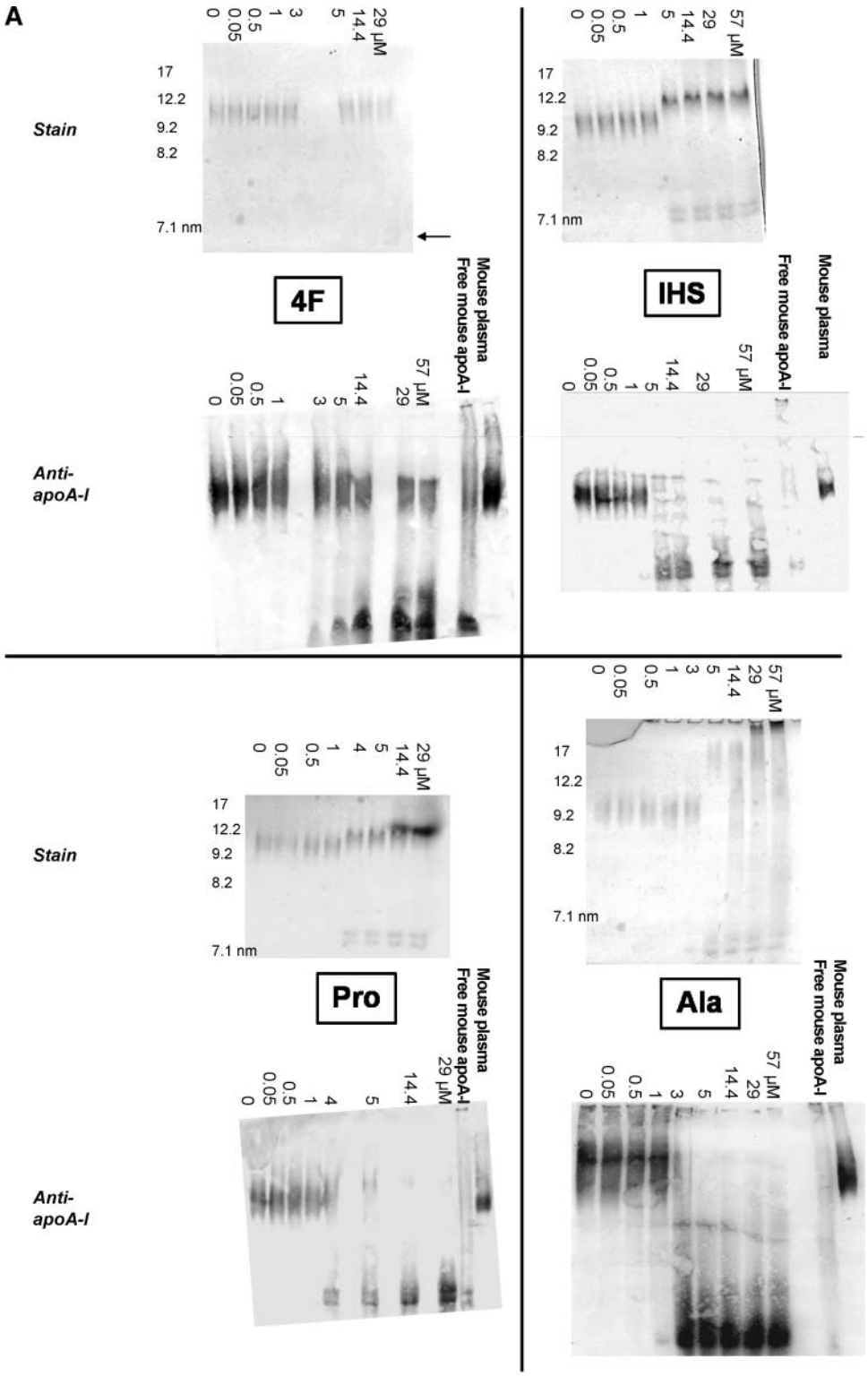

Fig. 3. Peptide-remodeled moHDL separated by native PAGE. Purified moHDL (34.3 μg/ml by protein) was incubated with increasing amounts of lipid-free peptide at 37°C for 20 min. A: Coomassie stain or anti-apoA-I immunoblot. Free apoA-I travels at ~7.1 nm, whereas mature moHDL is >10 nm diameter. B: The percent immunoreactivity of free apoA-I as a percentage of total apoA-I immunoreactivity per lane was determined by spot densitometry of immunoblots. Data is represented as mean ± SD.

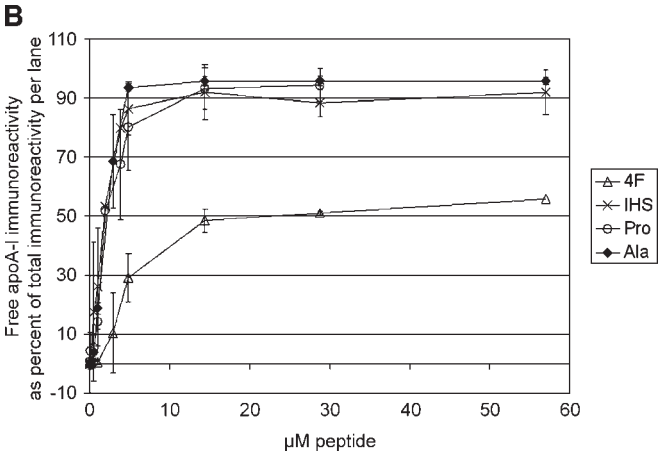

Fig. 3.—*Continued.*

With remodeling of moHDL by 4F, IHS, or Pro, apoA-II and the respective peptide remained in the HDL-density fractions (Fig. 4C). The unique lipoprotein with the density of a small LDL formed by Ala remodeling (Fig. 4A, B) contains apoA-II, the peptide, and a small amount of apoA-I (Fig. 4D).

ApoA-I mimetic peptides exceed apoA-I in their ability to accept ABCA1-mediated cholesterol efflux; tandem peptides are better than 4F

Macrophage foam cells exhibit upregulated membrane lipid transporters, including ABCA1 and ABCG1 (40), which can cause a net cholesterol efflux from the cell, a proven anti-atherosclerotic pathway (41, 42). Lipid-free apolipoproteins and synthetic amphipathic α-helical peptides can promote efflux of cellular cholesterol and phospholipid by binding to the unidirectional transporter ABCA1 (43–45). Tandem helical constructs based upon the sequence of human apoA-I helices show significantly increased cholesterol efflux compared with a single helix (46). Additionally, the proline-containing tandem helix domain of the apoE C terminus is required for efficient ABCA1 efflux and cannot be replicated by peptides representing individual helices from that domain (47). Finally, work with 18A-based peptides has shown that tandems linked by either proline or alanine cause more cholesterol efflux than an equal mass of monomeric 18A (48). Given these findings, the cholesterol efflux ability of the 4F-based tandem peptides as compared with monomeric 4F is of interest.

First, the IHS tandem peptide was compared with recombinant full-length apoA-I for the ability to efflux ^{3}H-labeled cholesterol from J774 foam cells (**Fig. 5A**). In untreated foam cells, IHS showed a 3.7-fold increase in percent efflux over apoA-I. With cAMP analog treatment to induce the expression of ABCA1, the tandem peptide showed a 2-fold increase. Both of these differences were statistically significant. On a per-molecule basis, the IHS tandem was 5.2-fold more concentrated than the mouse apoA-I, inasmuch as they were added at equal mass. However, adjusting this molar ratio for the five tandem helix pairs found in apoA-I shows the peptide to be at an equal tandem helix molarity. Therefore, the IHS tandem peptide exceeds the ABCA1-mediated efflux ability of full-length apoA-I on both a mass and tandem helix molar basis.

To compare the efflux abilities of monomeric versus tandem peptides, J774 cholesterol efflux was carried out as above. A range of concentrations of tandem peptide were compared with the monomeric 4F (Fig. 5B). The concentration dependence of the two proline-containing tandems (Pro and IHS) were hyperbolic for both their induced and uninduced concentration curves. Meanwhile, both induced and uninduced monomeric 4F show more linear concentration curves, with lower efflux than the tandem peptides at every concentration. At equal mass concentrations of tandem peptide and 4F, the tandem peptide is at roughly a 50% lower molar concentration.

Comparing separate efflux experiments after normalization to 4F showed no significant differences between IHS or Pro tandems in uninduced or induced cells. A direct comparison of the IHS and Ala tandems showed identical hyperbolic dose response for both peptides in both uninduced and induced cells (data not shown). In that experiment, no statistical differences were found, except for the highest concentration of peptide (25 μg/ml) in the induced cells; for that condition, the Ala tandem had 1.13-fold higher efflux than IHS ($P < 0.015$).

Cholesterol efflux was due to membrane transporters and not nonspecific membrane macropermeabilization, as no peptide-associated J774 macrophage cytotoxicity was detected by the 3-(4,5-dimethylthiazol-2-yl)-2,5-diphenyltetrazolium bromide (MTT) assay (data not shown).

The replacement of apoA-I on moHDL by mimetic peptide does not hinder the ability of the lipoprotein to accept cholesterol from ABCG1

As with ABCA1, ABCG1 is highly expressed in cholesterol-loaded macrophages. ABCG1 promotes cholesterol efflux from cells to HDL and other lipoprotein particles but not to lipid-free apoA-I (40). The displacement of apoA-I from HDL by apoA-I mimetic peptides could potentially influence ABCG1-mediated efflux to HDL.

At low peptide:moHDL concentration ratios, mimetic peptides can associate with HDL without significant displacement of apoA-I (data not shown). At higher concentrations, significant remodeling occurs, as shown above. The apolipoprotein content of HDL that optimizes ABCG1 efflux has not been identified. It could be the case that spherical HDL-sized particles are sufficient for maximal ABCG1 efflux regardless of their apoprotein content, inasmuch as ABCG1-dependent efflux does not appear to require the direct interaction of the transporter and lipoproteins (49). We determined the effect of apoA-I mimetic peptides present on moHDL in their role as cholesterol acceptors of ABCG1-mediated efflux, in both an apoA-I-rich and an apoA-I-poor HDL environment. Using BHK cells with a mifepristone-inducible huABCG1 gene, ABCG1-specific efflux was determined for five populations of moHDL: moHDL unmodified by peptide;

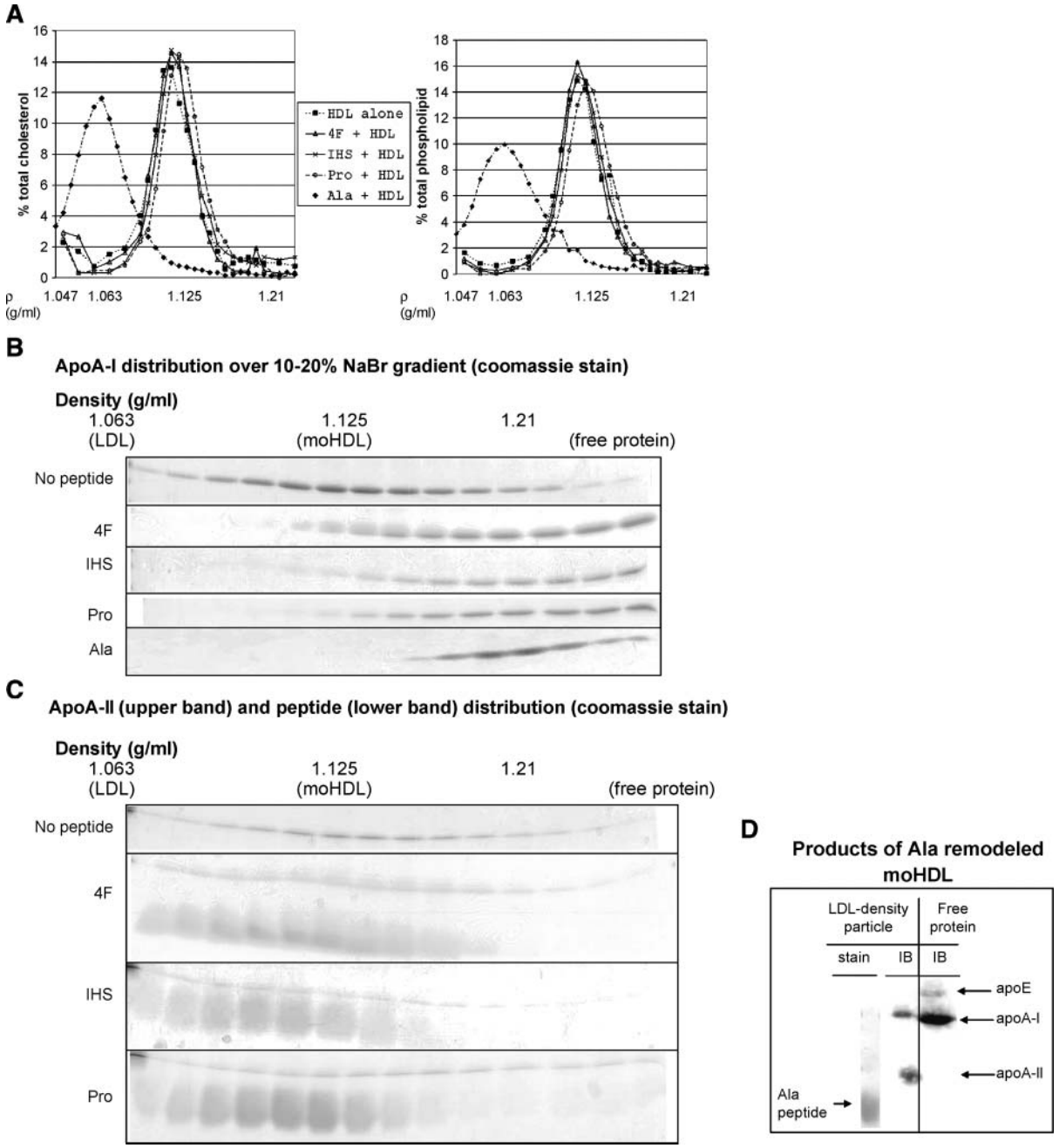

Fig. 4. Equilibrium density gradient separation of completely peptide-remodeled moHDL. moHDL at 0.237 mg/ml (protein) was incubated with 4F at a concentration of 182.3 μM, whereas all tandems were incubated at 33.67 μM. A: Cholesterol and phospholipid in density gradient fractions as a percent of total. B: Density distribution of apoA-I for control moHDL and after remodeling by 4F, IHS, Pro, and Ala peptides. C: Density distribution of apoA-II and peptide for those peptides that form moHDL-density particles (4F, IHS, Pro). D: Pooled fractions of Ala-remodeled moHDL representing small LDL and free protein densities. The fractions were either stained with Coomassie blue or immunoblotted (IB) for apoE, apoA-I, and apoA-II.

moHDL incubated with a low concentration of peptide (4F or IHS), leading to peptide association but not significant apoA-I displacement (peptide-associated); and moHDL incubated with a high concentration of peptide (4F or IHS), leading to peptide association and significant apoA-I displacement (peptide-remodeled). Because both simple HDL association as well as HDL remodeling may occur in a mouse after treatment with peptide, it is important to test the efflux ability of both populations relative to native moHDL. Peptide association or remodeling did not change moHDL density. The density fractions representing the cholesterol peak were pooled for all conditions.

In uninduced BHK cells, adding moHDL or peptide-modified moHDL at 10.2 μg cholesterol/ml caused a similar significant ($P < 0.02$) increase in the efflux of labeled cholesterol compared with control (**Fig. 6**). This is probably the result of the increase in simple aqueous

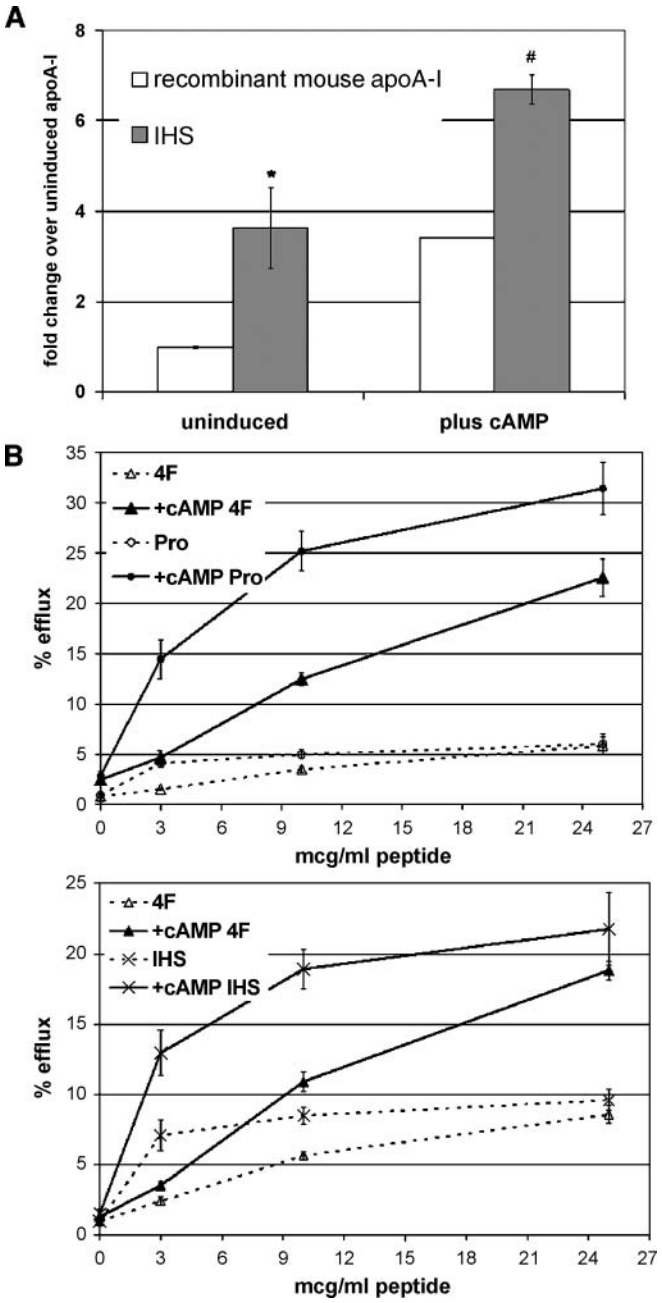

Fig. 5. Efflux of ^{3}H-cholesterol from J774 macrophage foam cells by lipid-free apoA-I mimetic peptides. A: The cholesterol efflux ability of the IHS tandem relative to lipid-free recombinant mouse apoA-I (both at 6 μg/ml) without (uninduced) or with CPT-cAMP. The comparison of IHS to apoA-I: * $P < 0.03$, # $P < 0.0025$. B: Representative independent experiments demonstrating the increased efflux ability of tandem peptides relative to monomeric 4F as a function of peptide concentration. Data is represented as mean ± SD.

diffusion due to the presence of a cholesterol acceptor in the medium.

Induction of ABCG1 expression in the transfected BHK cells with mifepristone led to significantly ($P < 0.03$) increased efflux to the moHDL and peptide-modified moHDL populations (Fig. 6). Adding a lesser amount of lipoprotein per well (2.6 μg cholesterol/ml) showed a dosimetric reduction in efflux (data not shown).

Though increasing the concentration of amphipathic α-helices increases ABCA1-dependent efflux (Fig. 5), it does not have the same effect on ABCG1-mediated efflux to HDL particles. The association of 4F or IHS with moHDL without the displacement of apoA-I does not affect the ABCG1 efflux-accepting capacity of the particle (Fig. 6). In contrast, moHDL exposed to levels of peptide high enough to displace most apoA-I had significantly ($P < 0.03$) higher efflux relative to unmodified moHDL. This demonstrates that either 4F or IHS on a moHDL particle is sufficient to replicate, and may exceed, the ABCG1-dependent efflux ability of the displaced apoA-I.

The increased efflux ability of the peptide-remodeled moHDLs, which have a 1.7-fold (4F) or 1.6-fold (IHS) increased protein:TC mass ratio relative to native moHDL, agrees with previous reports that protein-rich huHDL fractions have increased cholesterol efflux ability from foam cells (50).

Monomeric 4F better protects LDL from oxidation compared with tandem mimetic peptides

The anti-atherosclerotic effect of D4F in mice has been correlated with the reduction of LDL lipid peroxides (8). We therefore assessed the relative efficacy of the tandem peptides to inhibit LDL oxidation, compared with monomeric 4F. Oxidation of LDL was monitored by conjugated diene formation at OD 234nm. PUFAs contain bisallylic hydrogens, which are susceptible to radical abstraction. Radical abstraction, double-bond rearrangement to form a conjugated diene, and peroxide formation are all early steps in LDL oxidation, preceding formation of aldehydes or protein adducts (51).

The typical time course of conjugated diene formation during copper-mediated LDL oxidation involves *1*) a lag phase in which endogenous antioxidants are overcome, *2*) a linear phase in which the radical chain reaction occurs, and *3*) a plateau phase in which the oxidizable lipids have been expended (51). An effective anti-oxidant is defined as one that increases the lag time, decreases the slope, and decreases the total amount of LDL oxidation (51, 52). A representative 50 μM copper sulfate oxidation curve of purified moLDL (20 μg/ml, protein) is shown in **Fig. 7A**. Peptides were added at 10 μg/ml, a concentration experimentally determined to be the lowest effective dose of 4F (data not shown). In all three phases (lag time, slope, total oxidation) of the copper oxidation curve, 4F significantly decreased LDL oxidation (Fig. 7B). The proline-containing tandems (Pro and IHS) showed mixed anti-oxidative effects: neither could significantly increase the lag time, IHS alone could significantly decrease slope, and Pro alone could significantly decrease total oxidation. Interestingly, the Ala tandem appeared to act as a pro-oxidant; it did not have a significant effect on either lag time or slope, but it significantly increased the total oxidation of LDL. Another indication of the sequence specificity of the anti-oxidative effect was the potent reduction of lag time when an equal mass of BSA was added to the reaction instead of peptide (data not shown).

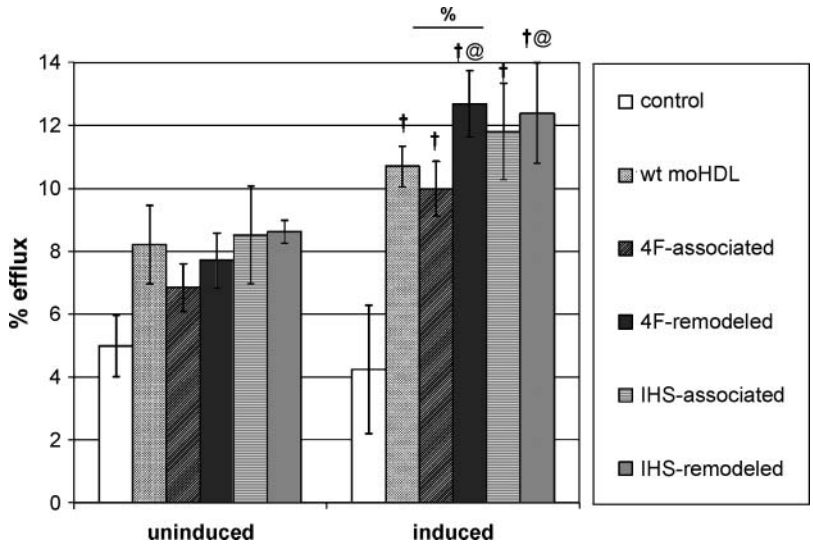

Fig. 6. Efflux of ^{3}H-cholesterol from human ABCG1-expressing (induced) and nonexpressing (uninduced) BHK cells by moHDL, peptide-associated moHDL, and completely peptide-remodeled moHDL (for preparation of these particles, see Methods). ABCG1 expression was induced by 10 nM mifepristone. Control was lipoprotein-free media. Lipoproteins were applied at 10.2 μg/ml total cholesterol. Statistical comparisons are as follows. Significant effect of induction † $P < 0.03$; with induced cells, comparison of moHDL versus peptide-altered moHDL @ $P < 0.03$; with induced cells, comparison of 4F-associated versus 4F-remodeled moHDL % $P < 0.005$. Data are represented as mean ± SD.

The influence of peptides on copper oxidation of LDL in the presence of HDL was also investigated. Adding 10 μg/ml HDL to 20 μg/ml LDL increased the conjugated diene lag time 2.5-fold, similar to that seen by Tribble et al. (53). The increase in lag time caused by HDL cannot be accounted for solely by the increase in lipid, inasmuch as independent experiments in which the LDL concentration (protein) was increased up to 1.5-fold did not show an appreciable increase in lag time, although total oxidation and slope were changed (data not shown). LDL + HDL + peptide oxidation (data not shown) demonstrated the same trends as LDL + peptide oxidation (Fig. 7A). Although the tandem peptides did not significantly change the oxidation reaction, compared with the control LDL + HDL incubation, the addition of 4F to the LDL + HDL was associated with an additional anti-oxidative effect.

We also investigated the ability of peptides to inhibit LDL oxidation, using the physiologic oxidant enzyme lipoxygenase (54, 55). LDL lipoxygenase oxidation does not demonstrate a lag phase, but a hyperbolic early phase and a linear propagation phase (Fig. 7C). In the case of lipoxygenase oxidation, all peptides except 4F significantly increased the slope of oxidation, compared with baseline (Fig. 7D). Oxidation in the presence of tandems Pro or Ala showed a significant increase, compared with 4F, with Ala showing a large 2.5-fold increase.

Combining the findings from copper and the more physiologic lipoxygenase oxidation of LDL shows the tandem peptides to be either ineffective or pro-oxidant, whereas 4F is shown to be either ineffective or anti-oxidant. Ultracentrifugation of an incubation of IHS (54.76 μg/ml) with or without moLDL (109.5 μg/ml) demonstrated that the peptide binds LDL, inasmuch as the peptide shifted from the free protein fractions to the LDL density fractions (data not shown).

DISCUSSION

We have investigated several apoA-I mimetic peptides that all share the 4F amphipathic α-helical backbone but differ in a variety of in vitro assays of potentially antiatherogenic processes. Any of the following properties could possibly influence the atheroprotective ability of mimetic peptides: lipid and HDL remodeling, protection of LDL from oxidation, and cholesterol efflux from cells mediated by ABCA1 and/or ABCG1. Here we have compared the relative efficacy of the single amphipathic α-helix with several tandem helix peptides for each of the above properties. Our results demonstrate that the relative efficacy of the individual peptides varies, depending on the parameter studied. This provides background for future investigation of the importance of each of these functions for in vivo atheroprotection. These studies will offer an important elucidation of the apoA-I mimetic peptide function(s) that best encompass their atheroprotective capacity.

The investigation of apoA-I mimetic peptides has provided important basic insights into the function of apoA-I (7), as well as the identification of a novel potential therapeutic for prevention of atherosclerosis (56). Navab and colleagues (26) have shown that oral D4F treatment decreases murine atherosclerotic lesion area, an effect that, correlated with increased pre-β HDL formation, in-

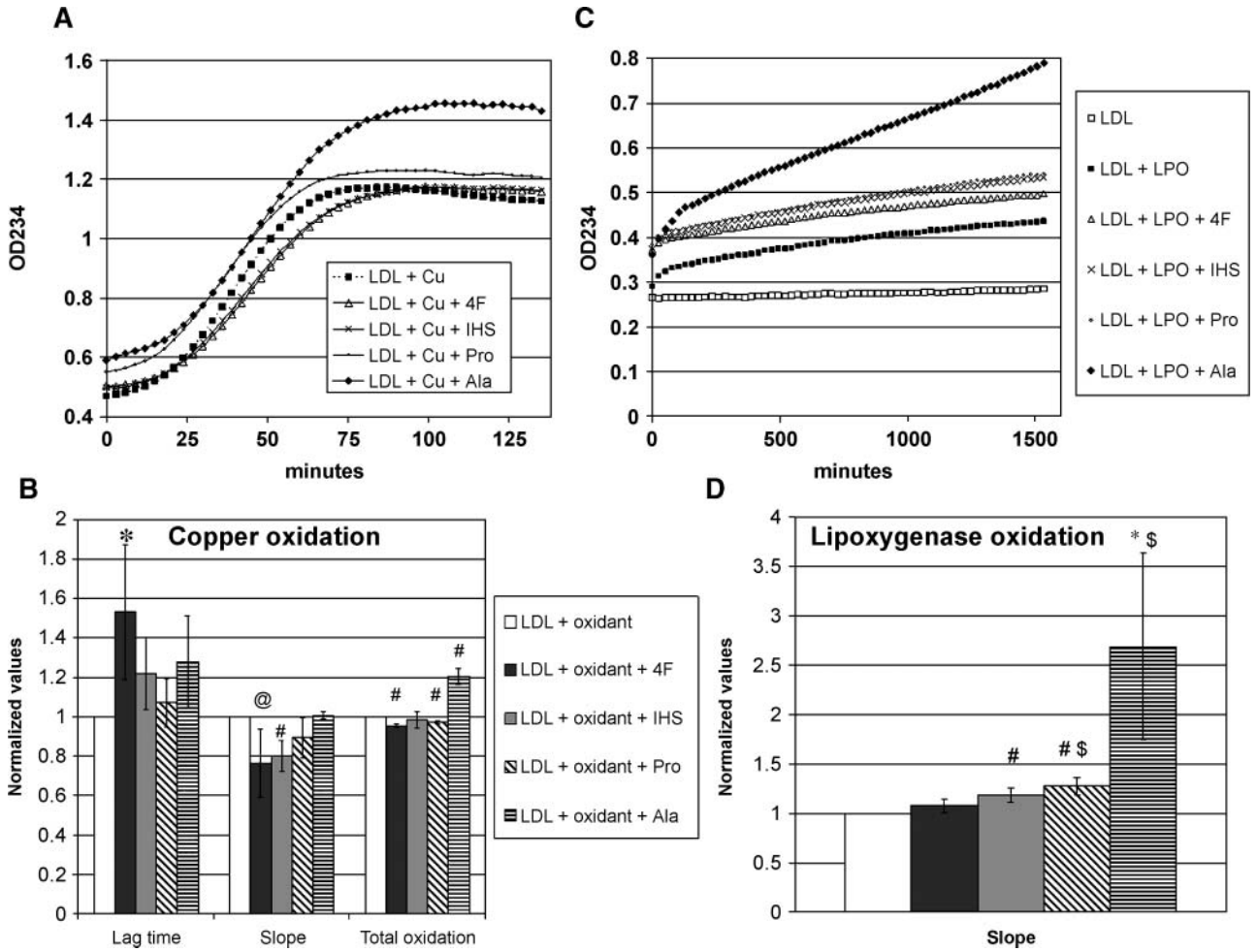

Fig. 7. Influence of peptides on mouse LDL (moLDL) oxidation. A: Representative copper sulfate (50 μM)-mediated oxidation of purified moLDL (20 μg/ml, protein) with or without added lipid-free peptide (10 μg/ml). This corresponds to 4.3, 1.9, 2.1, and 2.2 μM of 4F, IHS, Pro, and Ala, respectively. Monitored by conjugated diene formation (OD234). B: Quantitation of copper oxidation curves (n = 3). The lag time until linear oxidation phase, the slope of the linear oxidation phase, and the total increase in conjugated dienes over the course of the reaction are represented. C: Representative soybean lipoxygenase (300 U/ml)-mediated oxidation of purified moLDL (20 μg/ml) with or without added lipid-free peptide (10 μg/ml). Monitored by conjugated diene formation. D: Quantitation of lipoxygenase oxidation curves (n = 3). The slope of the linear oxidation phase is represented. Statistical comparison to oxidation without peptide: @ $P < 0.05$; * $P < 0.03$; # $P < 0.008$. Statistical comparison to oxidation with 4F: $ $P < 0.05$. Data is represented as mean ± SD.

creased cholesterol efflux and reduced lipoprotein oxidation. In this study, we have used in vitro assays of those correlated effects to determine the efficacy of related 4F-based peptides. We observed that the duplication of the α-helical 4F backbone in tandem peptides, as well as the linker used, modifies peptide behavior. Duplication of the peptide α-helical backbone increases moHDL remodeling ability and ABCA1 cholesterol efflux, but decreases ability to clear turbid lipid suspensions and protect moLDL from oxidation.

Peptides with a helix linker comprising a single proline (Pro) and a helix linker containing a proline in the context of an apoA-I IHS behaved very similarly in functional assays of turbid lipid suspension clearance, moHDL remodeling, ABCA1-mediated cholesterol efflux, and prevention of moLDL oxidation. This argues that the proline residue is the important functional unit of the 4/5 human apoA-I IHS in the context of apoA-I mimetic peptides. However, the two helix linkers do impart different peptide hydrophobicity (Table 1).

Although the proline-containing IHS linker behaved very similarly to the lone proline linker, a lone alanine linker quantitatively and qualitatively differed from the proline-containing tandems in several ways. The Ala tandem created unusually shaped DMPC-peptide particles and caused no net change in DMPC suspension turbidity (Fig. 1), created a small LDL-density particle when remodeling moHDL (Fig. 4), and increased total copper oxidation and rate of lipoxygenase oxidation of moLDL (Fig. 7). The ability of the alanine residue to propagate the helix and potentially create a straight 37 mer α-helix can potentially explain these experimental results. We hypothesize that the proline-containing tandem peptides adopt a bend roughly matching the radius of curvature of HDL. The Ala tandem, on the other hand, forms a long α-helix that does not form extensive rouleaux upon

interaction with DMPC, may cause particle fusion after HDL remodeling, and associates with LDL in a differential manner that increases the particles' susceptibility to oxidation. The preference of long α-helical peptides to bind larger lipoproteins (VLDL/LDL) has been described (57), and could explain the unique ability of Ala to remodel moHDL into LDL-sized particles.

The increased potency of the tandem peptides for moHDL remodeling, relative to 4F, has important implications for apoA-I mimetic peptides as potential therapeutics. The suggested correlation between peptide-mediated displacement of HDL apoA-I and prevention of atherosclerosis (8) implies that the peptides that can cause displacement at lower concentrations may offer a substantial therapeutic benefit. In addition, the difference in displacement behavior between tandem and monomeric peptides argues that the tandem helices found in full-length apoA-I are an important structural motif that may confer functional differences. The increased ability of a proline-kinked tandem apoA-I mimetic peptide to displace apoA-I from HDL, compared with a single 18-amino-acid amphipathic α-helix, has also been shown using 18A-based peptides by Chung et al. (14). Despite that previous work, it was important to confirm the increased efficacy of tandem mimetic peptides using the potent anti-atherosclerotic 4F backbone, which differs from 18A peptides because of both Leu→Phe replacements as well as terminal helix blocking.

Although helix number (i.e., tandem versus monomer) appears to be most influential on remodeling potency, the helix linker profoundly influences the structure of the remodeled spherical particle (Fig. 3A, Coomassie gels). With a proline-containing helix linker, a slightly larger HDL particle is formed after remodeling. With alanine, on the other hand, a much larger LDL-sized particle is created.

The concentration of mimetic peptide required for detectable remodeling of purified moHDL (1–5 μM), as detected by either agarose or native PAGE analysis, was roughly 10 times higher than the amount of D4F required to remodel HDL in whole human plasma (26). Given the identical methods of detection (immunoblot of native PAGE), there may be four possible explanations for this difference: *1*) Navab and colleagues used 30 min, rather than 20 min, at 37°C and thereby allowed the remodeling reaction to proceed further to completion; *2*) the antibody used by Navab and colleagues for immunoblotting may have been more sensitive; *3*) the presence of remodeling enzymes in whole human plasma may increase the potency of mimetic peptides; and/or *4*) the D-amino acid peptide is more effective than L-based peptides. The last possibility is unlikely, inasmuch as D- and L-based mimetic peptides have identical lipid surface affinity, circular dichroism, rat plasma half-lives, and cellular cholesterol efflux (15, 58). Stereochemical differences have only been shown to change the gastric degradation and urinary excretion of peptides (15, 26).

All four peptides generate pre-β migrating HDL when they remodel mature moHDL. This displacement has been described as a unique and valuable pathway for removal of lipid from atherosclerotic lesions (59). It has not been adequately appreciated that the other product of peptide-HDL remodeling is a peptide/apoA-II-containing cholesterol-rich particle. This resultant particle is always larger than untreated HDL, with 4F causing a small increase in particle diameter, Pro and IHS making large HDL-sized particles, and Ala making a small LDL-sized particle.

There is not a good understanding of the distribution of apoA-I and apoA-II on mouse HDL, although one review states that all moHDL is LpA-I/A-II (60). Therefore, these results argue for a selective displacement of apoA-I from LpA-I/A-II particles. After ultracentrifugal separation, the larger remodeled particle contains peptide and apoA-II, with little detectable apoA-I. Heat-induced HDL fusion is associated with the displacement of both apoA-I and apoA-II (61), whereas guanidinium chloride treatment of HDL is associated with selective loss of apoA-I and increased HDL size (62). ApoA-II could be stabilized on peptide-remodeled particles both by its inherent lipophilicity (63) or by forming salt bridges with peptide (64), inasmuch as 4F contains several Asp and Lys residues. The stabilization of apoA-II on peptide-remodeled HDL would probably be even greater in humans because, unlike in mice, human A-II forms cysteine-linked dimers that presumably have a larger hydrophobic area (65).

Proline- and alanine-containing tandem peptides similarly increased cholesterol efflux from J774 foam cells, as compared with monomeric 4F. This was the case for both uninduced and CPT-cAMP-induced cells. Uninduced J774 foam cells represent a model of the mouse atherosclerotic foam cell, with upregulated ABCA1 and ABCG1 transporters and consequently elevated efflux relative to a resting macrophage. Loading J774 or mouse peritoneal macrophages with acLDL increases cholesterol efflux (66) via upregulation of ABCA1- and ABCG1-derived efflux, not aqueous diffusion (67). Peptide-mediated cholesterol efflux from acLDL-loaded but uninduced J774 cells therefore models the efficacy of efflux that administered 4F versus tandem peptides are likely to be able to bring about from murine lesion foam cells. On the other hand, CPT-cAMP-induced J774 foam cells represent a specific supra-physiological induction of ABCA1. The difference between cholesterol efflux from uninduced and induced J774 foam cells is, therefore, ABCA1-specific.

Proline- and alanine-containing tandem peptides caused similarly increased ABCA1-mediated cholesterol efflux, as compared with monomeric 4F. This argues that the proline-containing helix kink is not required for efficient ABCA1 interaction, at least for tandem apoA-I mimetic peptides. It has been suggested that this motif is necessary for apoA-I–ABCA1 interaction and lipid efflux (68, 69). Our data do not support the correlation between peptide-mediated ABCA1-dependent efflux and DMPC clearance that has been described for full-length apoA-I. This suggests that apoA-I mimetic peptides do not require the same membrane-modifying steps for ABCA1-dependent efflux as does full-length apoA-I (34).

Our results suggest that the administration of apoA-I mimetic peptides may increase in vivo RCT in three ways. First, free peptide can interact with ABCA1 to bring about efficient cholesterol efflux; in fact, peptides are more potent than free apoA-I in this respect. Second, remodeling of moHDL by peptides displaces free apoA-I, which can accept cellular cholesterol efflux from ABCA1. Third, we have shown that a completely peptide-remodeled/apoA-II-containing moHDL is capable of greater ABCG1-dependent cholesterol efflux compared with apoA-I-rich unmodified moHDL. Whereas the first potential RCT mechanism can occur in the absence of HDL, the latter two require remodeling of HDL. Given the greater potency of tandem peptides for ABCA1 cholesterol efflux and moHDL remodeling compared with 4F, these RCT mechanisms are expected to be more active with tandem peptide treatment in vivo.

Previous studies showed human LpA-I/A-II effluxed less cellular cholesterol than LpA-I (60, 70). We report that the ABCG1-dependent cholesterol efflux to an apoA-I mimetic peptide/apoA-II-containing moHDL (apoA-I poor) was actually increased compared with unmodified moHDL (apoA-I-rich). Given the findings of the cited papers, the presence of peptide on moHDL may be more than just sufficient to replicate the efflux acceptance capacity of apoA-I and may in fact have greater acceptance capacities than apoA-I. This may be due to peptides counterbalancing the detrimental efflux effect of relative apoA-II enrichment of the moHDL.

Our original hypothesis was that displacement of apoA-I from HDL by peptides could potentially create a lipoprotein dysfunctional for cholesterol efflux, potentially limiting RCT from the atherosclerotic lesion. Others have shown that HDL with a decreased apoA-I/apoA-II ratio has decreased efflux ability from SR-BI high-expressing Fu5AH cells (71). However, the ABCG1 in vitro efflux data we present confirms ABCG1 efflux as a viable pathway for prevention of atherosclerosis in mimetic peptide-treated mice. Peptide modification of HDL does not decrease its ability to accept cholesterol from ABCG1, and may in fact increase the efflux acceptance capacity if significant amounts of apoA-I mimetic peptide are present.

Pro-inflammatory oxidative modification of LDL is an important initiator of macrophage foam cell formation and the subsequent formation of the atheroma (72). We demonstrate that 4F inhibits in vitro LDL oxidation in all phases of copper oxidation and does not increase LDL oxidation by lipoxygenase. None of the tandem peptides could match this ability. We hypothesize that the mechanism of oxidation protection by mimetic peptides is by binding to the lipoprotein and blocking access to the oxidation-prone acyl tails in the lipid milieu. The cofractionation of a tandem peptide (IHS) with LDL after ultracentrifugation suggests that the peptides can bind LDL, though HDL can outcompete this binding. Peptide binding to LDL could provide some protection against oxidation at the stage of transition from aqueous to lipid phase (copper), as suggested by Bielicki and Oda (73), or block binding of the pro-oxidant enzyme (lipoxygenase). Although tandem peptides are well-suited to binding HDL because of the particle's small radius of curvature, we suggest that they bind the larger lipoprotein LDL with a worse fit that does not protect against oxidant access and may even increase that access in the case of the Ala tandem. On the other hand, 4F possesses a single amphipathic α-helix that we hypothesize can interact with all lipoproteins as if they were planar.

The use of a tandem peptide that shows greater ABCA1-dependent efflux could increase RCT at the same time that it increases the removal of oxidized lipids from the arterial wall (74). Depending upon the subsequent movement of these removed oxidized lipids, that removal could be pro- or anti-atherogenic.

It could be possible that remodeled HDL particles with a reduced apoA-I/A-II ratio could be more prone to oxidation, or not as able to prevent LDL oxidation (38). However, a preliminary experiment using equal amounts of particle (by protein) showed that apoA-I-poor Ala-remodeled moHDL had an increased copper oxidation lag time compared with unmodified moHDL (data not shown).

We initially hypothesized that tandem peptides, which better match the basic unit of lipid-associated apoA-I structure, would uniformly exceed 4F in these in vitro assays. However, 4F and tandem peptides show differing abilities in these assays of potentially anti-atherosclerotic processes. Future testing of these peptides in appropriate murine models of atherosclerosis may show some of these processes to be consistently vital for inhibition of atherosclerosis. However, the caveat of potential peptide-specific mechanisms of atheroprotection cannot be disregarded.

The authors thank Dr. Timothy Sontag for the recombinant mouse apoA-I protein, comparison of apoA-I and peptide cholesterol efflux abilities, technical assistance with DMPC clearance assays, and valuable scientific discussions. Dr. Kristi Lazar synthesized the IHS peptide and, along with Hélène Miller-Auer and Dr. Stephen Meredith, provided much-appreciated technical assistance with the preparation of synthetic peptides, as well as valuable scientific discussions. Yimei Chen assisted with electron microscopy studies. The authors also thank Jack Oram for the ABCG1-expressing BHK cells.

REFERENCES

1. Newton, R. S., and B. R. Krause. 2002. HDL therapy for the acute treatment of atherosclerosis. *Atheroscler.* **3 (Suppl.):** 31–38.
2. Gordon, D. J., J. L. Probstfield, R. J. Garrison, J. D. Neaton, W. P. Castelli, J. D. Knoke, D. R. Jacobs, Jr., S. Bangdiwala, and H. A. Tyroler. 1989. High-density lipoprotein cholesterol and cardiovascular disease. Four prospective American studies. *Circulation.* **79:** 8–15.
3. Linsel-Nitschke, P., and A. R. Tall. 2005. HDL as a target in the treatment of atherosclerotic cardiovascular disease. *Nat. Rev. Drug Discov.* **4:** 193–205.
4. Eriksson, M., L. A. Carlson, T. A. Miettinen, and B. Angelin. 1999. Stimulation of fecal steroid excretion after infusion of recombinant proapolipoprotein A-I: potential reverse cholesterol transport in humans. *Circulation.* **100:** 594–598.

5. Nissen, S. E., T. Tsunoda, E. M. Tuzcu, P. Schoenhagen, C. J. Cooper, M. Yasin, G. M. Eaton, M. A. Lauer, W. S. Sheldon, C. L. Grines, et al. 2003. Effect of recombinant apoA-I Milano on coronary atherosclerosis in patients with acute coronary syndromes: a randomized controlled trial. *J. Am. Med. Assoc.* **290:** 2292–2300.
6. Li, W. H., M. Tanimura, C. C. Luo, S. Datta, and L. Chan. 1988. The apolipoprotein multigene family: biosynthesis, structure, structure-function relationships, and evolution. *J. Lipid Res.* **29:** 245–271.
7. Anantharamaiah, G. M., V. K. Mishra, D. W. Garber, G. Datta, S. P. Handattu, M. N. Palgunachari, M. Chaddha, M. Navab, S. T. Reddy, J. P. Segrest, et al. 2007. Structural requirements for antioxidative and anti-inflammatory properties of apolipoprotein A-I mimetic peptides. *J. Lipid Res.* **48:** 1915–1923.
8. Navab, M., G. M. Anantharamaiah, S. T. Reddy, S. Hama, G. Hough, V. R. Grijalva, A. C. Wagner, J. S. Frank, G. Datta, D. Garber, et al. 2004. Oral D-4F causes formation of pre-beta high-density lipoprotein and improves high-density lipoprotein-mediated cholesterol efflux and reverse cholesterol transport from macrophages in apolipoprotein E-null mice. *Circulation.* **109:** 3215–3220.
9. Navab, M., G. M. Anantharamaiah, S. Hama, D. W. Garber, M. Chaddha, G. Hough, R. Lallone, and A. M. Fogelman. 2002. Oral administration of an apo A-I mimetic peptide synthesized from D-amino acids dramatically reduces atherosclerosis in mice independent of plasma cholesterol. *Circulation.* **105:** 290–292.
10. Ou, J., Z. Ou, D. W. Jones, S. Holzhauer, O. A. Hatoum, A. W. Ackerman, D. W. Weihrauch, D. D. Gutterman, K. Guice, K. T. Oldham, et al. 2003. L-4F, an apolipoprotein A-1 mimetic, dramatically improves vasodilation in hypercholesterolemia and sickle cell disease. *Circulation.* **107:** 2337–2341.
11. Garber, D. W., G. Datta, M. Chaddha, M. N. Palgunachari, S. Y. Hama, M. Navab, A. M. Fogelman, J. P. Segrest, and G. M. Anantharamaiah. 2001. A new synthetic class A amphipathic peptide analogue protects mice from diet-induced atherosclerosis. *J. Lipid Res.* **42:** 545–552.
12. Boguski, M. S., M. Freeman, N. A. Elshourbagy, J. M. Taylor, and J. I. Gordon. 1986. On computer-assisted analysis of biological sequences: proline punctuation, consensus sequences, and apolipoprotein repeats. *J. Lipid Res.* **27:** 1011–1034.
13. Anantharamaiah, G. M., J. L. Jones, C. G. Brouillette, C. F. Schmidt, B. H. Chung, T. A. Hughes, A. S. Bhown, and J. P. Segrest. 1985. Studies of synthetic peptide analogs of the amphipathic helix. Structure of complexes with dimyristoyl phosphatidylcholine. *J. Biol. Chem.* **260:** 10248–10255.
14. Chung, B. H., G. M. Anatharamaiah, C. G. Brouillette, T. Nishida, and J. P. Segrest. 1985. Studies of synthetic peptide analogs of the amphipathic helix. Correlation of structure with function. *J. Biol. Chem.* **260:** 10256–10262.
15. Garber, D. W., Y. V. Venkatachalapathi, K. B. Gupta, J. Ibdah, M. C. Phillips, J. B. Hazelrig, J. P. Segrest, and G. M. Anantharamaiah. 1992. Turnover of synthetic class A amphipathic peptide analogues of exchangeable apolipoproteins in rats. Correlation with physical properties. *Arterioscler. Thromb.* **12:** 886–894.
16. Borhani, D. W., D. P. Rogers, J. A. Engler, and C. G. Brouillette. 1997. Crystal structure of truncated human apolipoprotein A-I suggests a lipid-bound conformation. *Proc. Natl. Acad. Sci. USA.* **94:** 12291–12296.
17. Wang, G., J. T. Sparrow, and R. J. Cushley. 1997. The helix-hinge-helix structural motif in human apolipoprotein A-I determined by NMR spectroscopy. *Biochemistry.* **36:** 13657–13666.
18. Ajees, A. A., G. M. Anantharamaiah, V. K. Mishra, M. M. Hussain, and H. M. K. Murthy. 2006. Crystal structure of human apolipoprotein A-I: insights into its protective effect against cardiovascular diseases. *Proc. Natl. Acad. Sci. USA.* **103:** 2126–2131.
19. Roberts, L. M., M. J. Ray, T. W. Shih, E. Hayden, M. M. Reader, and C. G. Brouillette. 1997. Structural analysis of apolipoprotein A-I: limited proteolysis of methionine-reduced and -oxidized lipid-free and lipid-bound human apo A-I. *Biochemistry.* **36:** 7615–7624.
20. Rogers, D. P., C. G. Brouillette, J. A. Engler, S. W. Tendian, L. Roberts, V. K. Mishra, G. M. Anantharamaiah, S. Lund-Katz, M. C. Phillips, and M. J. Ray. 1997. Truncation of the amino terminus of human apolipoprotein A-I substantially alters only the lipid-free conformation. *Biochemistry.* **36:** 288–300.
21. Wang, G. 2002. How the lipid-free structure of the N-terminal truncated human apoA-I converts to the lipid-bound form: new insights from NMR and X-ray structural comparison. *FEBS Lett.* **529:** 157–161.
22. Martin, D. D. O., M. S. Budamagunta, R. O. Ryan, J. C. Voss, and M. N. Oda. 2006. Apolipoprotein A-I assumes a "looped belt" conformation on reconstituted high density lipoprotein. *J. Biol. Chem.* **281:** 20418–20426.
23. Wu, Z., M. A. Wagner, L. Zheng, J. S. Parks, J. M. Shy III, J. D. Smith, V. Gogonea, and S. L. Hazen. 2007. The refined structure of nascent HDL reveals a key functional domain for particle maturation and dysfunction. *Nat. Struct. Mol. Biol.* **14:** 861–868.
23a. Carnemolla, R., X. Ren, T. K. Biswas, S. C. Meredith, C. A. Reardon, J. Wang, and G. S. Getz. 2008. The specific amino acid sequence between helices 7 and 8 influences the binding specificity of human apolipoprotein A-I for HDL subclasses: a potential for HDL preferential generation. *J. Biol. Chem.* doi:10.1074.
24. Brouillette, C. G., G. M. Anantharamaiah, J. A. Engler, and D. W. Borhani. 2001. Structural models of human apolipoprotein A-I: a critical analysis and review. *Biochim. Biophys. Acta.* **1531:** 4–46.
25. Lazar, K. L., H. Miller-Auer, G. S. Getz, J. P. Orgel, and S. C. Meredith. 2005. Helix-turn-helix peptides that form alpha-helical fibrils: turn sequences drive fibril structure. *Biochemistry.* **44:** 12681–12689.
26. Navab, M., G. M. Anantharamaiah, S. T. Reddy, S. Hama, G. Hough, V. R. Grijalva, N. Yu, B. J. Ansell, G. Datta, D. W. Garber, et al. 2005. Apolipoprotein A-I mimetic peptides. *Arterioscler. Thromb. Vasc. Biol.* **25:** 1325–1331.
27. Basu, S. K., J. L. Goldstein, G. W. Anderson, and M. S. Brown. 1976. Degradation of cationized low density lipoprotein and regulation of cholesterol metabolism in homozygous familial hypercholesterolemia fibroblasts. *Proc. Natl. Acad. Sci. USA.* **73:** 3178–3182.
28. Goldstein, J. L., Y. K. Ho, S. K. Basu, and M. S. Brown. 1979. Binding site on macrophages that mediates uptake and degradation of acetylated low density lipoprotein, producing massive cholesterol deposition. *Proc. Natl. Acad. Sci. USA.* **76:** 333–337.
29. Cabana, V. G., J. N. Siegel, and S. M. Sabesin. 1989. Effects of the acute phase response on the concentration and density distribution of plasma lipids and apolipoproteins. *J. Lipid Res.* **30:** 39–49.
30. Liu, L., A. E. Bortnick, M. Nickel, P. Dhanasekaran, P. V. Subbaiah, S. Lund-Katz, G. H. Rothblat, and M. C. Phillips. 2003. Effects of apolipoprotein A-I on ATP-binding cassette transporter A1-mediated efflux of macrophage phospholipid and cholesterol: formation of nascent high density lipoprotein particles. *J. Biol. Chem.* **278:** 42976–42984.
31. Vaughan, A. M., and J. F. Oram. 2005. ABCG1 redistributes cell cholesterol to domains removable by high density lipoprotein but not by lipid-depleted apolipoproteins. *J. Biol. Chem.* **280:** 30150–30157.
32. Sankararamakrishnan, R., and S. Vishveshwara. 1990. Conformational studies on peptides with proline in the right-handed alpha-helical region. *Biopolymers.* **30:** 287–298.
33. Datta, G., M. Chaddha, S. Hama, M. Navab, A. M. Fogelman, D. W. Garber, V. K. Mishra, R. M. Epand, R. F. Epand, S. Lund-Katz, et al. 2001. Effects of increasing hydrophobicity on the physical-chemical and biological properties of a class A amphipathic helical peptide. *J. Lipid Res.* **42:** 1096–1104.
34. Vedhachalam, C., P. T. Duong, M. Nickel, D. Nguyen, P. Dhanasekaran, H. Saito, G. H. Rothblat, S. Lund-Katz, and M. C. Phillips. 2007. Mechanism of ATP-binding cassette transporter A1-mediated cellular lipid efflux to apolipoprotein A-I and formation of high density lipoprotein particles. *J. Biol. Chem.* **282:** 25123–25130.
35. Mishra, V. K., G. M. Anantharamaiah, J. P. Segrest, M. N. Palgunachari, M. Chaddha, S. W. Sham, and N. R. Krishna. 2006. Association of a model class A (apolipoprotein) amphipathic alpha helical peptide with lipid: high resolution NMR studies of peptide-lipid discoidal complexes. *J. Biol. Chem.* **281:** 6511–6519.
36. Rye, K. A., and P. J. Barter. 2004. Formation and metabolism of prebeta-migrating, lipid-poor apolipoprotein A-I. *Arterioscler. Thromb. Vasc. Biol.* **24:** 421–428.
37. Kunitake, S. T., C. M. Mendel, and L. K. Hennessy. 1992. Interconversion between apolipoprotein A-I-containing lipoproteins of pre-beta and alpha electrophoretic mobilities. *J. Lipid Res.* **33:** 1807–1816.
38. Navab, M., S. Y. Hama, C. J. Cooke, G. M. Anantharamaiah, M. Chaddha, L. Jin, G. Subbanagounder, K. F. Faull, S. T. Reddy, N. E. Miller, et al. 2000. Normal high density lipoprotein inhibits

three steps in the formation of mildly oxidized low density lipoprotein: step 1. *J. Lipid Res.* **41:** 1481–1494.
39. Chapman, M. J., S. Goldstein, D. Lagrange, and P. M. Laplaud. 1981. A density gradient ultracentrifugal procedure for the isolation of the major lipoprotein classes from human serum. *J. Lipid Res.* **22:** 339–358.
40. Oram, J. F., and A. M. Vaughan. 2006. ATP-binding cassette cholesterol transporters and cardiovascular disease. *Circ. Res.* **99:** 1031–1043.
41. Out, R., M. Hoekstra, K. Habets, I. Meurs, V. de Waard, R. B. Hildebrand, Y. Wang, G. Chimini, J. Kuiper, T. J. C. Van Berkel, et al. 2008. Combined deletion of macrophage ABCA1 and ABCG1 leads to massive lipid accumulation in tissue macrophages and distinct atherosclerosis at relatively low plasma cholesterol levels. *Arterioscler. Thromb. Vasc. Biol.* **28:** 258–264.
42. Yvan-Charvet, L., M. Ranalletta, N. Wang, S. Han, N. Terasaka, R. Li, C. Welch, and A. R. Tall. 2007. Combined deficiency of ABCA1 and ABCG1 promotes foam cell accumulation and accelerates atherosclerosis in mice. *J. Clin. Invest.* **117:** 3900–3908.
43. von Eckardstein, A., J. R. Nofer, and G. Assmann. 2001. High density lipoproteins and arteriosclerosis. Role of cholesterol efflux and reverse cholesterol transport. *Arterioscler. Thromb. Vasc. Biol.* **21:** 13–27.
44. Oram, J. F., and J. W. Heinecke. 2005. ATP-binding cassette transporter A1: a cell cholesterol exporter that protects against cardiovascular disease. *Physiol. Rev.* **85:** 1343–1372.
45. Van Eck, M., I. S. T. Bos, W. E. Kaminski, E. Orso, G. Rothe, J. Twisk, A. Bottcher, E. S. Van Amersfoort, T. A. Christiansen-Weber, W-P. Fung-Leung, et al. 2002. Leukocyte ABCA1 controls susceptibility to atherosclerosis and macrophage recruitment into tissues. *Proc. Natl. Acad. Sci. USA.* **99:** 6298–6303.
46. Natarajan, P., T. M. Forte, B. Chu, M. C. Phillips, J. F. Oram, and J. K. Bielicki. 2004. Identification of an apolipoprotein A-I structural element that mediates cellular cholesterol efflux and stabilizes ATP binding cassette transporter A1. *J. Biol. Chem.* **279:** 24044–24052.
47. Vedhachalam, C., V. Narayanaswami, N. Neto, T. M. Forte, M. C. Phillips, S. Lund-Katz, and J. K. Bielicki. 2007. The C-terminal lipid-binding domain of apolipoprotein E is a highly efficient mediator of ABCA1-dependent cholesterol efflux that promotes the assembly of high-density lipoproteins. *Biochemistry.* **46:** 2583–2593.
48. Mendez, A. J., G. M. Anantharamaiah, J. P. Segrest, and J. F. Oram. 1994. Synthetic amphipathic helical peptides that mimic apolipoprotein A-I in clearing cellular cholesterol. *J. Clin. Invest.* **94:** 1698–1705.
49. Wang, N., D. Lan, W. Chen, F. Matsuura, and A. R. Tall. 2004. ATP-binding cassette transporters G1 and G4 mediate cellular cholesterol efflux to high-density lipoproteins. *Proc. Natl. Acad. Sci. USA.* **101:** 9774–9779.
50. Ohta, T., K. Saku, K. Takata, R. Nakamura, Y. Ikeda, and I. Matsuda. 1995. Different effects of subclasses of HDL containing apoA-I but not apoA-II (LpA-I) on cholesterol esterification in plasma and net cholesterol efflux from foam cells. *Arterioscler. Thromb. Vasc. Biol.* **15:** 956–962.
51. Jialal, I., and S. Devaraj. 1996. Low-density lipoprotein oxidation, antioxidants, and atherosclerosis: a clinical biochemistry perspective. *Clin. Chem.* **42:** 498–506.
52. Frei, B., and J. M. Gaziano. 1993. Content of antioxidants, preformed lipid hydroperoxides, and cholesterol as predictors of the susceptibility of human LDL to metal ion-dependent and -independent oxidation. *J. Lipid Res.* **34:** 2135–2145.
53. Tribble, D. L., B. M. Chu, E. L. Gong, F. van Venrooij, and A. V. Nichols. 1995. HDL antioxidant effects as assessed using a non-exchangeable probe to monitor particle-specific peroxidative stress in LDL-HDL mixtures. *J. Lipid Res.* **36:** 2580–2589.
54. Folcik, V. A., R. A. Nivar-Aristy, L. P. Krajewski, and M. K. Cathcart. 1995. Lipoxygenase contributes to the oxidation of lipids in human atherosclerotic plaques. *J. Clin. Invest.* **96:** 504–510.
55. Navab, M., S. Y. Hama, G. M. Anantharamaiah, K. Hassan, G. P. Hough, A. D. Watson, S. T. Reddy, A. Sevanian, G. C. Fonarow, and A. M. Fogelman. 2000. Normal high density lipoprotein inhibits three steps in the formation of mildly oxidized low density lipoprotein: steps 2 and 3. *J. Lipid Res.* **41:** 1495–1508.
56. Li, X., K. Y. Chyu, J. R. Faria Neto, J. Yano, N. Nathwani, C. Ferreira, P. C. Dimayuga, B. Cercek, S. Kaul, and P. K. Shah. 2004. Differential effects of apolipoprotein A-I-mimetic peptide on evolving and established atherosclerosis in apolipoprotein E-null mice. *Circulation.* **110:** 1701–1705.
57. Nikoulin, I. R., and L. K. Curtiss. 1998. An apolipoprotein E synthetic peptide targets to lipoproteins in plasma and mediates both cellular lipoprotein interactions in vitro and acute clearance of cholesterol-rich lipoproteins in vivo. *J. Clin. Invest.* **101:** 223–234.
58. Remaley, A. T., F. Thomas, J. A. Stonik, S. J. Demosky, S. E. Bark, E. B. Neufeld, A. V. Bocharov, T. G. Vishnyakova, A. P. Patterson, T. L. Eggerman, et al. 2003. Synthetic amphipathic helical peptides promote lipid efflux from cells by an ABCA1-dependent and an ABCA1-independent pathway. *J. Lipid Res.* **44:** 828–836.
59. Curtiss, L. K., D. T. Valenta, N. J. Hime, and K-A. Rye. 2006. What is so special about apolipoprotein AI in reverse cholesterol transport? *Arterioscler. Thromb. Vasc. Biol.* **26:** 12–19.
60. Tailleux, A., P. Duriez, J. C. Fruchart, and V. Clavey. 2002. Apolipoprotein A-II, HDL metabolism and atherosclerosis. *Atherosclerosis.* **164:** 1–13.
61. Jayaraman, S., D. L. Gantz, and O. Gursky. 2006. Effects of salt on the thermal stability of human plasma high-density lipoprotein. *Biochemistry.* **45:** 4620–4628.
62. Pownall, H. J., B. D. Hosken, B. K. Gilliard, C. L. Higgins, H. Y. Lin, and J. B. Massey. 2007. Speciation of human plasma high-density lipoprotein (HDL): HDL stability and apolipoprotein A-I partitioning. *Biochemistry.* **46:** 7449–7459.
63. Gilliard, B. K., H. S. Courtney, J. B. Massey, and H. J. Pownall. 2007. Serum opacity factor unmasks human plasma high-density lipoprotein instability via selective delipidation and apolipoprotein A-I desorption. *Biochemistry.* **46:** 12968–12978.
64. Rye, K-A., K. Wee, L. K. Curtiss, D. J. Bonnet, and P. J. Barter. 2003. Apolipoprotein A-II inhibits high density lipoprotein remodeling and lipid-poor apolipoprotein A-I formation. *J. Biol. Chem.* **278:** 22530–22536.
65. Blanco-Vaca, F., J. C. Escolà-Gil, J. M. Martín-Campos, and J. Julve. 2001. Role of apoA-II in lipid metabolism and atherosclerosis: advances in the study of an enigmatic protein. *J. Lipid Res.* **42:** 1727–1739.
66. Zanotti, I., F. Potì, E. Favari, K. R. Steffensen, J. A. Gustafsson, and F. Bernini. 2006. Pitavastatin effect on ATP binding cassette A1-mediated lipid efflux from macrophages: evidence for liver X receptor (LXR)-dependent and LXR-independent mechanisms of activation by cAMP. *J. Pharmacol. Exp. Ther.* **317:** 395–401.
67. Adorni, M. P., F. Zimetti, J. T. Billheimer, N. Wang, D. J. Rader, M. C. Phillips, and G. H. Rothblat. 2007. The roles of different pathways in the release of cholesterol from macrophages. *J. Lipid Res.* **48:** 2453–2462.
68. Chroni, A., T. Liu, I. Gorshkova, H. Y. Kan, Y. Uehara, A. von Eckardstein, and V. I. Zannis. 2003. The central helices of apoA-I can promote ATP-binding cassette transporter A1 (ABCA1)-mediated lipid efflux. Amino acid residues 220–231 of the wild-type apoA-I are required for lipid efflux in vitro and high density lipoprotein formation in vivo. *J. Biol. Chem.* **278:** 6719–6730.
69. Svidirov, D., A. Hoang, W. Huang, and J. Sasaki. 2002. Structure-function studies of apoA-I variants: site-directed mutagenesis and natural mutations. *J. Lipid Res.* **43:** 1283–1292.
70. Castro, G., L. P. Nihoul, C. Dengremont, C. de Geitere, B. Delfly, A. Tailleux, C. Fievet, N. Duverger, P. Denefle, J. C. Fruchart, et al. 1997. Cholesterol efflux, lecithin-cholesterol acyltransferase activity, and pre-beta particle formation by serum from human apolipoprotein A-I and apolipoprotein A-I/apolipoprotein A-II transgenic mice consistent with the latter being less effective for reverse cholesterol transport. *Biochemistry.* **36:** 2243–2249.
71. Fournier, N., A. Cogny, V. Atger, D. Pastier, D. Goudouneche, A. Nicoletti, N. Moatti, J. Chambaz, J. L. Paul, and A. D. Kalopissis. 2002. Opposite effects of plasma from human apolipoprotein A-II transgenic mice on cholesterol efflux from J774 macrophages and Fu5AH hepatoma cells. *Arterioscler. Thromb. Vasc. Biol.* **22:** 638–643.
72. Glass, C. K., and J. L. Witztum. 2001. Atherosclerosis. the road ahead. *Cell.* **104:** 503–516.
73. Bielicki, J. K., and M. N. Oda. 2002. Apolipoprotein A-I(Milano) and apolipoprotein A-I(Paris) exhibit an antioxidant activity distinct from that of wild-type apolipoprotein A-I. *Biochemistry.* **41:** 2089–2096.
74. Reddy, S. T., S. Hama, C. Ng, V. Grijalva, M. Navab, and A. M. Fogelman. 2002. ATP-binding cassette transporter 1 participates in LDL oxidation by artery wall cells. *Arterioscler. Thromb. Vasc. Biol.* **22:** 1877–1883.